Astronomy reports

Millimetre observations of circumstellar disks around the young stars TW Hya and HD 100546

D. Wilner, T. Bourke (CfA, USA); C. Wright (ADFA); J. Jörgensen, E. van Dishoeck (Leiden, The Netherlands); T. Wong (ATNF)

Many young stars exhibit emission from circumstellar dust disks with properties similar to the early Solar System. Observations at millimetre wavelengths are especially important for characterising the physical properties of these disks because the disk material beyond a few stellar radii is at temperatures ranging from a few tens to a few hundreds of degrees, and the physical and chemical conditions can be probed in detail in this part of the spectrum.

The recent upgrade of the Compact Array with receivers for the 3-mm atmospheric window provides a new opportunity for high resolution imaging of protoplanetary disks located in the southern sky. We have observed the dust continuum and HCO^+ ($J = 1 – 0$) line emission at 89 GHz (3.4 mm) from two young southern disk targets, TW Hya, the closest known classical T Tauri star, and HD 100546, a nearby Herbig Be star whose infrared spectrum shows crystalline silicates, indicative of comet-like dust. These were observed using two compact antenna configurations of three antennas, with an angular resolution of about two arcseconds.

TW Hya is isolated from any molecular cloud but retains a face-on disk visible in scattered light that extends to a radius of at least 3.5 arcseconds, equivalent to a linear size of approximately 200 astronomical units (AU). Its disk has been detected in a number of molecular lines at submillimetre wavelengths using single dish telescopes. Modelling all available data suggests the TW Hya disk is substantially evolved, with indications of significant particle growth, i.e., evolution toward planet-sized objects.

HD 100546 is a nearby Herbig Be star and shows a disk-like scattered light distribution of substantial size, about 8 arcseconds (8,000 AU), as well as strong millimetre emission from dust. Mid-infrared spectroscopy shows remarkably strong crystalline silicate bands, similar to those observed in comet Hale-Bopp and indicative of substantial processing of the dust within the disk.

Figure 12 shows the 89 GHz continuum emission detected from TW Hya and HD 100546. The flux observed from TW Hya agrees well with expectations from its spectral energy distribution. Models that reproduce the far-infrared emission of HD 100546 using only an extended envelope do not account for the flux observed at 1.2 mm which suggests that a circumstellar disk component must be present in the system. The Compact Array observations provide the first direct evidence for this compact disk component.

Figure 13 shows the HCO$^+$ ($J = 1 - 0$) spectrum of TW Hya, integrated over the continuum position. The velocity and line-width of the narrow emission line are in agreement with single dish observations. The HCO$^+$ ($J = 1 - 0$) line emission from the TW Hya disk is spatially resolved, with a fitted Gaussian size of 3.2 arcseconds. Since the critical density of the HCO$^+$ ($J = 1 - 0$) line for collisional excitation is approximately 6 x 10^4 cm^{-3}, the detection of extended emission indicates high densities must be present to large radii, independent of any detailed physical and chemical model for the disk. No HCO$^+$ ($J = 1 - 0$) emission was detected toward HD 100546, a surprising result. Observations of the more abundant species CO in the 110 – 115 GHz range are needed.

Previous modelling of the TW Hya disk suggests that species like CO and HCO$^+$ are depleted due to a combination of photodissociation in the warm surface layers and freezing-out in the cold parts of the disk shielded from stellar activity. These models, based either on a radiatively-heated accretion disk structure or a passive two-layer disk structure, are consistent with the Compact Array observations, for both the size scale and the absolute intensity of the HCO$^+$ line. The models all have disk masses of 0.03 solar masses and disk radii of 200 AU. High depletion has been observed in other young disks of varying size and indicates that substantial depletion occurs throughout the disk, as expected for planet formation through accretion.
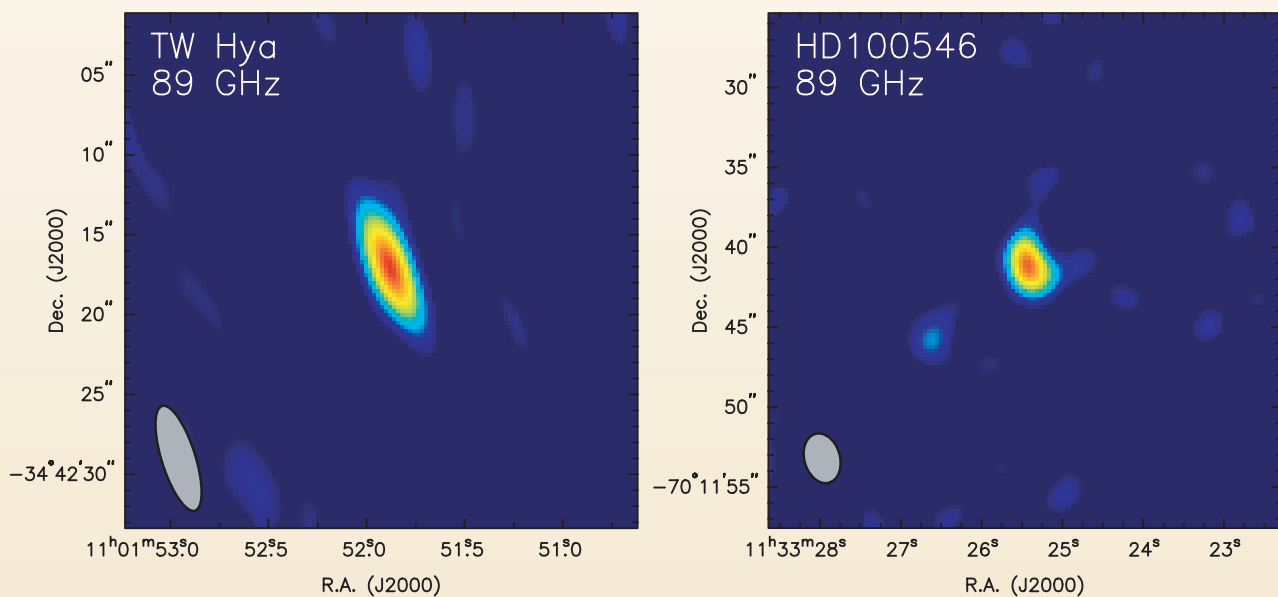
Figure 12 *Images obtained with the Compact Array showing radio continuum emission at 89 GHz from the young stars TW Hya and HD 100546.*
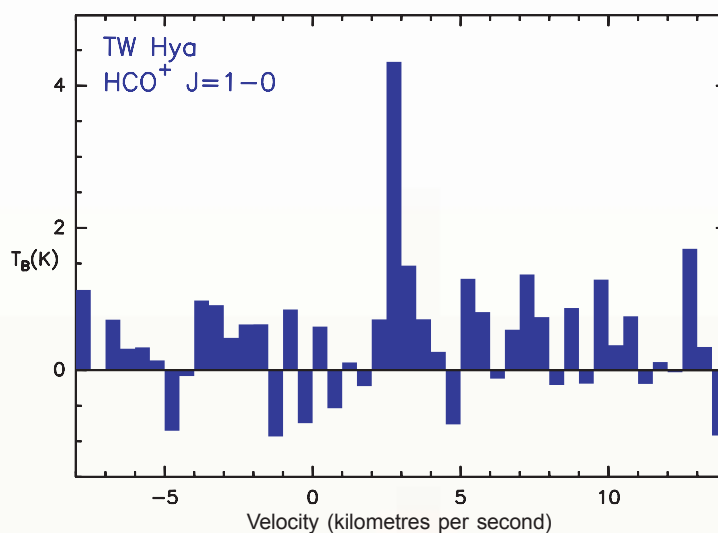
Figure 13 *HCO⁺ spectrum of TW Hya showing the detection of a narrow emission line centred at a velocity of 3 kilometres per second.*

Imaging HCN emission around R Scl

T. Wong (ATNF); F. L. Schoeier (Leiden Obseratory, The Netherlands & Stockholm Observatory, Sweden); M. Lindqvist, H. Olofsson (Stockholm Observatory, Sweden)

One of the first targets for the Compact Array 3-mm system was the carbon-rich red giant star R Sculptoris, which is believed to be encircled by a detached shell of molecular gas and dust. For a dying star to be losing mass in a slow stellar wind is quite typical, but the presence of a thin detached shell indicates that at some point in the past there was a sudden increase in the rate of mass loss, perhaps due to the sudden onset of helium shell burning. By observing molecular emission in the shell at high angular resolution, one can determine not only the expansion velocity of the shell, but also the time scale of the mass-loss variation (related to the shell thickness) and the degree of isotropy of the wind (related to the symmetry of the shell). Notwithstanding their scientific interest, circumstellar shells also make ideal "test sources" for the current 3-mm system because they are relatively simple structures of small angular size (compared, for instance, to molecular clouds).

Although the previous single-dish observations that had indicated the presence of a shell around R Scl were made in a CO emission line with the Swedish-ESO Submillimetre Telescope (SEST), the Compact Array's restricted frequency range led us to observe the HCN $(J = 1 - 0)$ line at 88.6 GHz. We observed R Scl in several compact configurations of three antennas, with baselines ranging from 31 – 413 m, between June and October 2002. We found that the HCN emission is extremely compact, with a Gaussian full width at half maximum (FWHM) of about one arcsecond, so that even our high-resolution imaging only partially resolves the source (Figure 14). The total Compact Array flux is consistent with the SEST flux within the calibration uncertainties. Thus, it appears that the HCN emission is associated with an attached envelope resulting from recent mass loss rather than the older (and hence larger) detached shell inferred from the CO data. The difference in geometry is corroborated by higher-transition, single-dish HCN spectra, which indicate that the HCN envelope is expanding more slowly than the bulk of the CO emission. The lack of HCN in the detached shell is most likely due to its photodissociation into CN, as has been observed in several other sources.

A detailed radiative transfer code, based on the Monte Carlo method, has been used to jointly model the Compact Array and single-dish HCN data. The main inputs to the model are the current mass-loss rate (in solar masses per year) and the stellar radiation field. With reasonable assumptions for these, we have calculated the best-fit values for the HCN abundance (relative to H_2) and envelope size, using the HCN data (both single-dish and interferometer) as constraints. The best-fit envelope size is about 1,000 AU, whereas modelling the Compact Array data alone yields a size of only 300 AU (comparable to the size of the emission region in our high-resolution maps). Thus a single set of model parameters cannot simultaneously fit both the single-dish and interferometer data. Possibly the high optical depth of the HCN lines makes the emission very sensitive to changes in the physical conditions of the inner envelope (such as clumping in the mass distribution) that are not accounted for in our model.
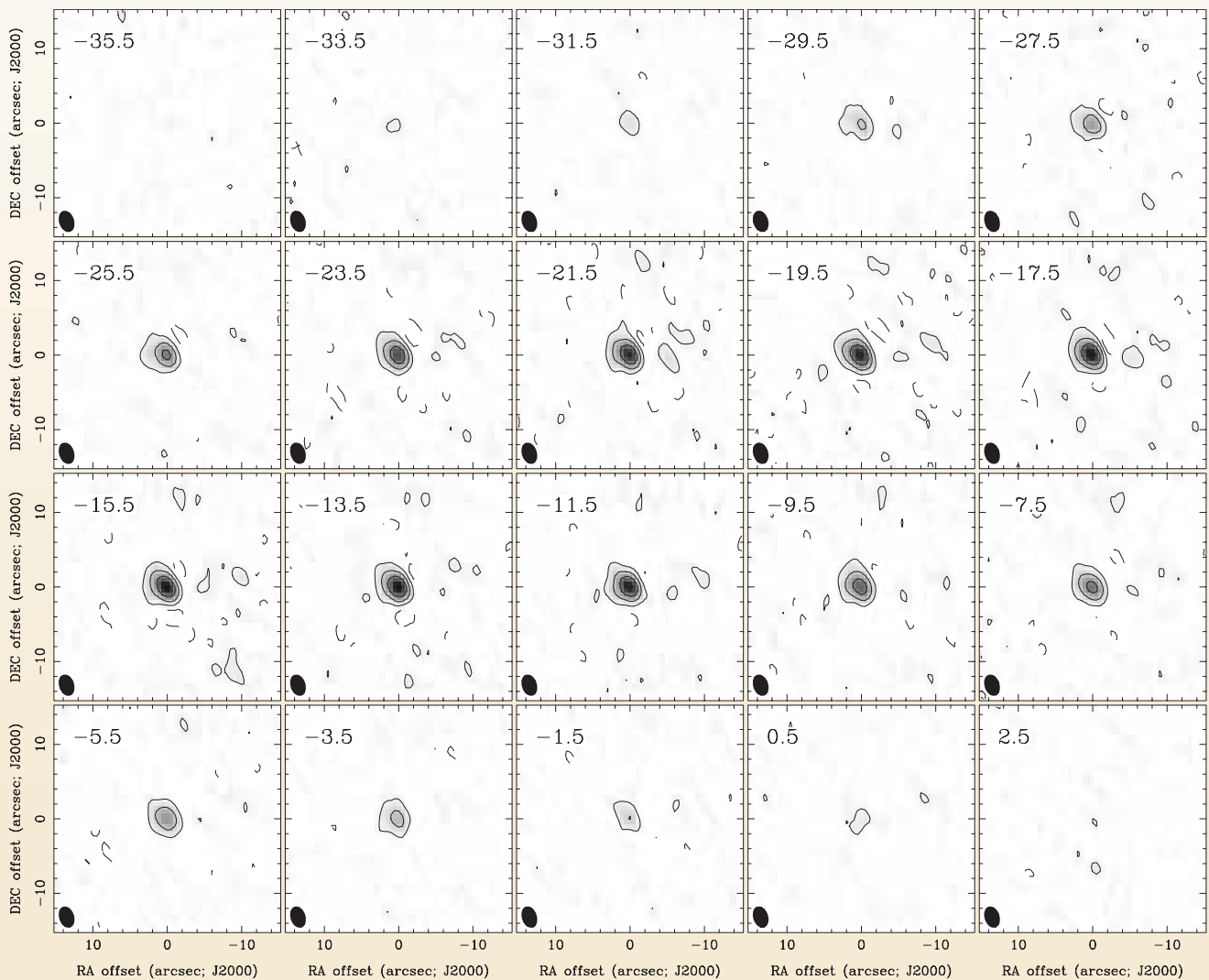
Figure 14 Channel maps of HCN (J =1 – 0) emission from R Scl. The beam size is 2.7 x 1.8 arcseconds. The velocity channels (given relative to the local standard of rest) have been binned to 2 kilometres per second.

Planetary nebulae and butterfly wings

R. Deacon (University of Sydney); J. Chapman (ATNF); A. Green (University of Sydney)

Planetary nebulae are the remnants of low-to-middle mass stars. When stars, like our own Sun, run out of core-burning hydrogen, they go through a sequence of structural changes. The outer layers greatly expand while the stellar cores decrease in size and become hotter. Of particular interest in the "giant" stages is that most stars shed a large fraction of their mass through slow, dense stellar winds. Such winds transfer more than half of a star's original mass back into the interstellar medium. After most of the outer layers of gas have been blown away, stars change from losing mass in slow dense winds to losing mass in hot, low-density, fast winds. The hot winds sweep up the remaining material surrounding the stars and the swept-up shells may then be seen as glowing ionised nebulae. Stars in this stage are known as planetary nebulae.

Planetary nebulae can be spectacularly beautiful and reveal many different forms. While some appear circular, others have the shapes of butterfly wings, or show elliptical or bipolar shapes, in some cases with complex, filamentary structures. The causes for this proliferation of geometries are not yet known, but several different theories are being debated. One possible explanation is that magnetic fields from the stars constrain the stellar winds to flow in some directions only. Alternatively, companion stars or planets may cause gravitational effects, or rotation of the central stars may be important.

We are studying a sample of stars that are the immediate precursors to planetary nebulae. These stars are known as post-asymptotic giant branch (post-AGB) stars and have evolved beyond the second giant phase known as the AGB. The different geometries seen in planetary nebulae are also seen in post-AGB stars and it seems likely that the shaping of non-spherical planetary nebulae winds begins early in the post-AGB phase of stellar evolution. By studying the post-AGB stars we may be able to determine what causes the butterfly-wing geometries and other complicated structures seen in some planetary nebulae.

To investigate this question, we have selected a well-defined sample of 85 post-AGB stars from a previous study of OH maser sources in the Galactic plane (Sevenster et al.). For this sample, we are observing radio emission from hydroxyl, water and silicon monoxide molecules that are located in the outflowing stellar winds. Each molecule requires different physical conditions to exist and provides information on the physical gas conditions in a layer around the central star. The radiation from these molecules is produced by a maser effect—the microwave equivalent of lasers. The maser spectra also provide accurate information on the wind speeds, and on whether the winds are likely to be spherically symmetrical or distorted.

Figure 15 shows examples of OH maser spectra, for sources in our sample, at a frequency of 1612 MHz. We have classified the spectra using six different categories, depending on the shape of the spectral profiles. Of the 85 sources, 57 exhibit a classic double-peaked spectrum ("D-type") at 1612 MHz, with steep outer edges and sloping inner edges between the two peaks. This spectral profile is characteristic of an expanding spherical shell, with the two peaks being emitted from small "caps" on the front and rear of the shell. In our sample we see several variations on the classic double-peaked profiles: The "De" spectra have one emission peak which is very much stronger than the other—this shows that the maser emission is much stronger on one side of the star than on the other. The "Dw" stars have OH 1612-MHz spectra with sloping outer edges as well as sloping inner edges. These are expected to be stars with bipolar shells. More unusual is the "DD" source with four emission peaks. Only one other source with this characteristic is known.

In our sample we also find five "S-type" sources. These show only a single peak of maser emission, but otherwise have characteristics in common with AGB and post-AGB stars. Finally the "I" or irregular spectra have multiple emission peaks and a larger than usual velocity range. Post-AGB stars with such irregular spectra are usually associated with exotic envelope geometries.

From our maser data, together with still-to-come measurements of the stellar magnetic fields and detailed radio images of the outflowing winds, we hope to clarify why some stars evolve to have asymmetric winds and others do not.
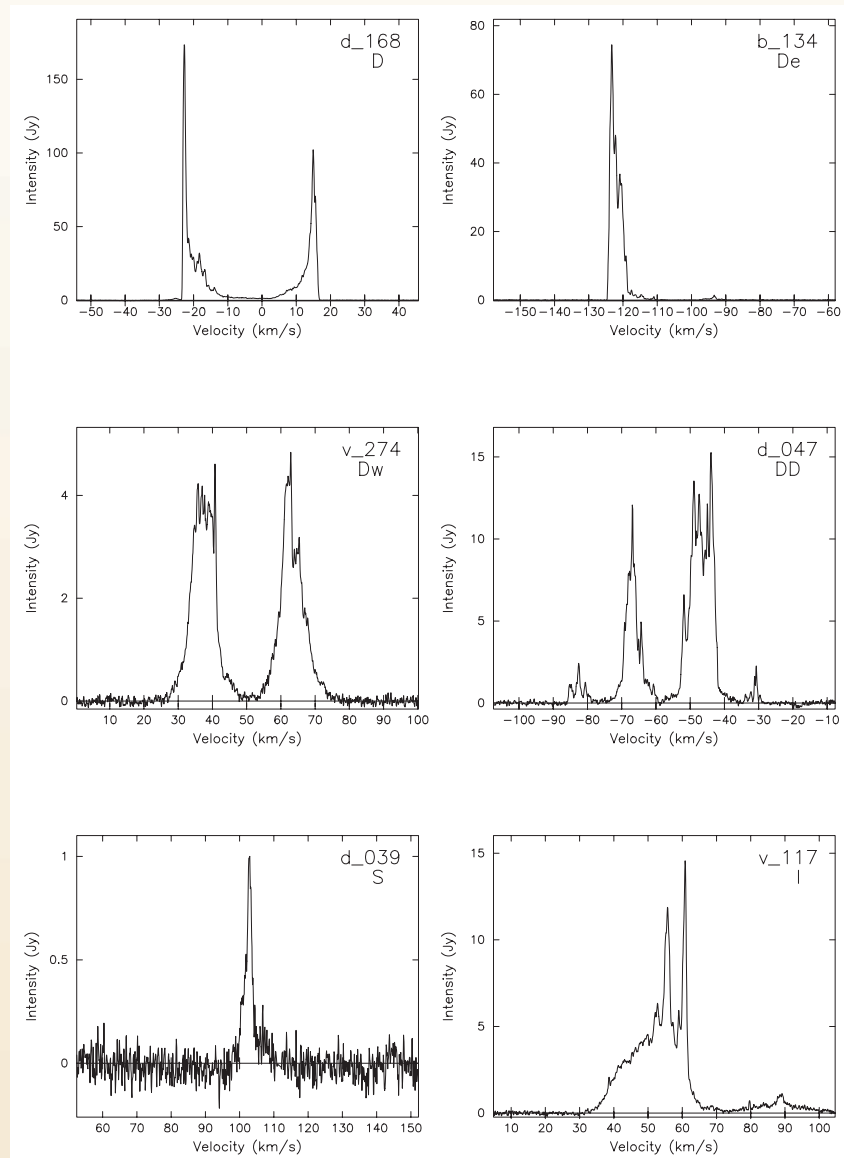
Figure 15 *Some examples of OH 1612 MHz spectra of post-AGB stars, obtained from data taken with the Parkes radio telescope in September 2002. The catalog name of each star is given in the top right-hand corner with a category type given below the name. The 85 stars in this study have been classified into six different types depending on whether the OH maser profiles are double (D, De, Dw and DD-types), single (S-type) or irregular (I-type).*

Figure 16 M2-9 is a striking example of a "butterfly" or bipolar planetary nebula. This image, taken with the Hubble Space Telescope, shows a pair of high-speed "jets" of gas moving away from the centre of the nebula at super-sonic velocities of more than 300 kilometres per second.

Photo credit: B. Balick (University of Washington, USA); V. Icke (Leiden University, The Netherlands); G. Mellema (Stockholm University, Sweden); NASA (USA)

Image reference: Image STScI-PRC1997-38

The Compact Array captures a "baby" supernova

S. Ryder (Anglo-Australian Observatory); R. Subrahmanyan (ATNF); E. Sadler (University of Sydney); K. Weiler (Naval Research Laboratory, USA)

On the evening of 10 December 2001, the Rev. Robert Evans was conducting his regular supernova patrol from his backyard in the Blue Mountains west of Sydney, when he came across an interloper in the nearby late-type spiral galaxy NGC 7424. In an era when the vast majority of supernova discoveries are made by robotic telescopes, or as part of the high-redshift supernova search programs, Evans' trained eye, photographic memory, and trusty 12-inch telescope have allowed him to maintain a proud record of supernova discoveries. Supernova 2001ig was his 39th discovery, and the 241st supernova discovery of 2001.

Since its commissioning, the Compact Array has played a leading role in the monitoring of several supernovae at radio wavelengths, most notably SN 1987A and SN 1978K. Radio emission from Type II supernovae is typically not detected (or even searched for) until weeks, months, or even years after the outburst. On the evening of Saturday 15 December 2001, we made use of six hours of unallocated time on the Compact Array to make images of SN 2001ig at frequencies of 8.6, 4.8, 2.5 and 1.4 GHz. Somewhat to our surprise, there was a positive detection at the highest frequencies. On New Year's Eve, it was detected at 18.8 GHz using the prototype 12-mm receiver system on three Compact Array antennas.

Figure 17 shows an image of the field at 4.8 GHz from Compact Array observations taken on 17 February 2002. SN 2001ig is the upper of the two bright sources shown as contours; the source to the southwest is an unrelated background source. Figure 18 shows the results from our Compact Array monitoring program; for clarity, only the 8.6 and 4.8 GHz data are shown. The radio "light curve" of a supernova can be divided into three phases—a rapid turn-on with a steep spectral index, due in large part to a decrease in the line-of-sight absorption; a peak in the flux density which is first seen at the higher frequencies; a more gradual decline in an optically-thin phase. By March 2002, SN 2001ig had begun to fade at 5 and 8 GHz, but then abruptly doubled in flux and remained that way for three weeks, before resuming its decline. In late August, it again briefly halted its decline. Such dramatic excursions from a smooth decline are rare, and generally thought to be associated with the interaction of the blast ejecta with a dense and rather inhomegenous circumstellar medium.

SN 2001ig is one of only a half dozen or so known examples of a "Type IIb" supernova, in which the hydrogen lines seen in their early optical spectra soon fade away, suggesting that much of their outer layers were shed before the star exploded. Two possible mechanisms for this, which could also account for the bumps in the radio light curve, are thermal pulses due to carbon/helium flashes in the core of a 5 – 10 solar mass asymptotic giant branch progenitor star, occurring on periodic time scales of around 500 years, or a modulation of a red supergiant progenitor wind due to eccentric orbital motion about a massive binary companion, leading to a pinwheel-like clumping in the circumstellar medium. Efforts are now underway to model the observed behaviour in the context of these scenarios, while Compact Array monitoring of SN 2001ig will continue throughout 2003.
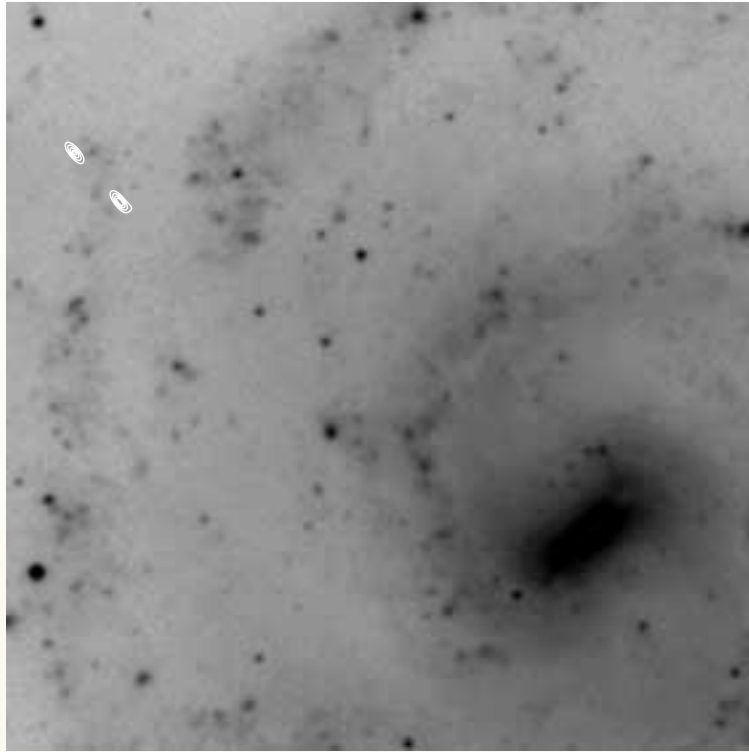
Figure 17 Contours showing the 4.8-GHz radio emission from the region around SN2001ig, overlaid on an image of the outskirts of the galaxy NGC 7424 from the Digitized Sky Survey. SN2001ig is upper left of the two radio sources. The lower radio source is an unrelated background source.
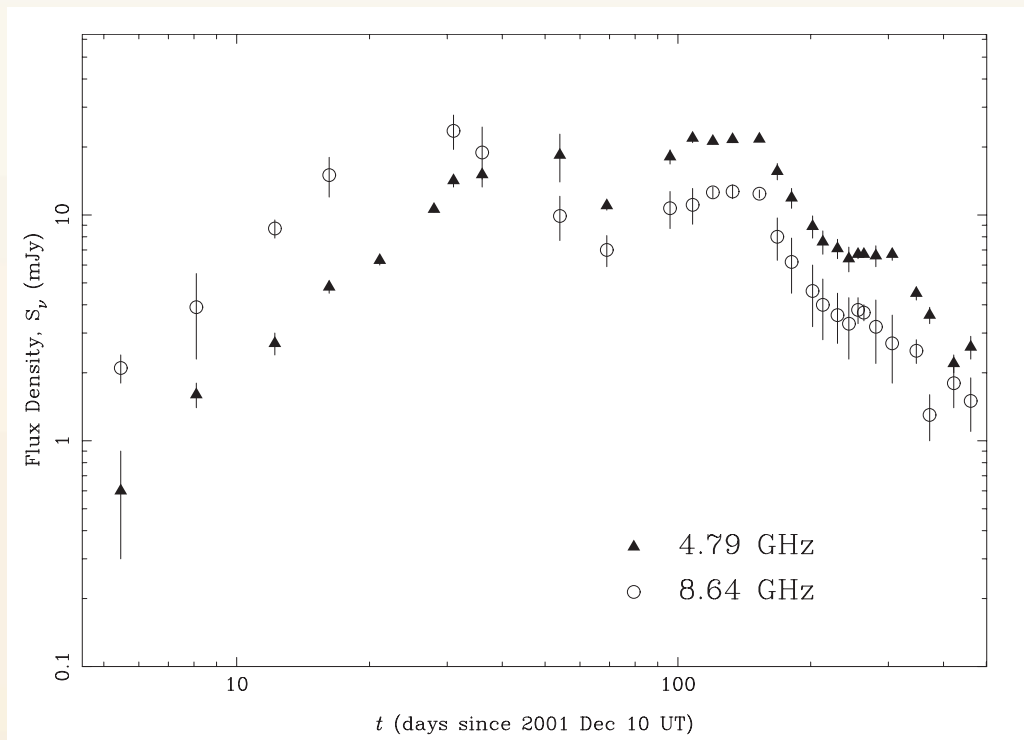
Figure 18 The radio light curve of SN2001ig, showing the change in intensity of the radio emission at frequencies of 4.8 and 8.6 GHz over a period of approximately 400 days.

Pulsar discoveries at Parkes

F. Camilo (Columbia University, USA); B. M. Gaensler (Harvard University, USA); D. R. Lorimer (University of Manchester, UK); R. N. Manchester (ATNF)

2002 yielded a remarkable vintage of young pulsar discoveries, with the Parkes telescope playing a central role.

Young pulsars are objects of interest for a variety of reasons. The physics of core collapse in evolved stars can be inferred from observations which provide the initial spin period, space velocity, and magnetic field distributions of neutron stars, while measurements of their beaming properties, luminosities, and spectra are crucial for determining the Galactic population and birthrate of pulsars. Young pulsars frequently exhibit period glitches, and emit substantial amounts of X- and gamma rays—these can be observed to learn about the internal composition of neutron stars, and the pulse emission mechanisms. In addition, young neutron stars are embedded in compact non-thermal radio and/or X-ray pulsar wind nebulae where the ambient medium confines the relativistic pulsar wind, or otherwise interact with their host supernova remnants. The embedded pulsars are unique probes of their immediate environment and the local interstellar medium.

A natural location to search for young pulsars is the Galactic plane and more specifically in supernova remnants. However, establishing bona fide associations between Galactic pulsars and supernova remnants has been a painfully slow business: two were known by 1970 (those of the Crab and Vela), five by 1985, and only 10 by 2000, although more than 200 supernova remnants and 1,400 pulsars are known. Searches for associations have not been immensely productive in this regard—a survey of 88 supernova remnants in the 1990s netted zero associated pulsars!

More recently the Parkes multibeam pulsar survey of the Galactic plane, using a 13-beam receiver system at a frequency of 1,400 MHz, covered a very large area with sensitivity broadly comparable to that of the best previous surveys of supernova remnants. This survey has been extraordinarily successful, discovering approximately 700 pulsars, but to date has yielded only one new association between a pulsar and a supernova remnant (for a discussion of this pulsar, PSR J1119–6127, in the supernova remnant G292.2–0.5 see the ATNF Annual Report 2000).

We have used a method to detect young pulsars that relies on the premise that the existence of a pulsar wind nebula must also indicate the presence of an energetic and reasonably young pulsar. We decided to search pulsar wind nebulae *as deeply as possible*, to look for new detections of young pulsars. A complication with this approach is that it is not always clear whether a particular compact object is a pulsar wind nebula. However, recent X-ray images from the *Chandra* X-ray Observatory can, in some cases, unambiguously identify a pulsar wind nebula and its embedded pulsar even when pulsations are not detected.

One such example is provided by the beautiful *Chandra* observation of SNR G292.0+1.8, shown in Figure 19. The X-ray data of this source reveal a two arcminute pulsar wind nebula within which is located a point source. While this supernova remnant had been searched previously without a pulsar detection, the *Chandra* results encouraged new efforts. In a 10-hour integration at Parkes using the central beam of the multibeam system, we detected PSR J1124–5916, with a pulse period of 135 milliseconds, a moderate dispersion measure (330 pc cm^{-3}), and a characteristic age of 2,900 years. PSR J1124–5916 is a *very weak* source, with a flux density at 1,400 MHz of 80 microJansky and a low radio luminosity. X-ray pulsations were detected subsequent to and with the help of the radio discovery.

Following this discovery, many more pulsar wind nebulae were searched as deeply as possible with the Arecibo, Green Bank, Jodrell Bank and Parkes telescopes. In all, six very weak and energetic young pulsars, associated with wind nebulae (in some cases within supernovae), have been detected in the past two years, and the searches continue. The newly discovered objects are being investigated in follow-up studies at radio and X-ray wavelengths, and a careful analysis of the sensitivity and selection effects relevant to these searches is underway and should yield useful constraints on the combination of luminosity distribution and beaming fraction of young pulsars.

Our study has shown that many young pulsars beam towards the Earth. However, many of them do so with luminosities that are detectable with the best present-day radio telescopes only when using integration times of a day or so, if at all! While X-ray astronomers have long been used to spending a day obtaining a handful of photons from astronomical sources of interest, such as young pulsars, this is a relatively new lesson for radio pulsar observers to learn.
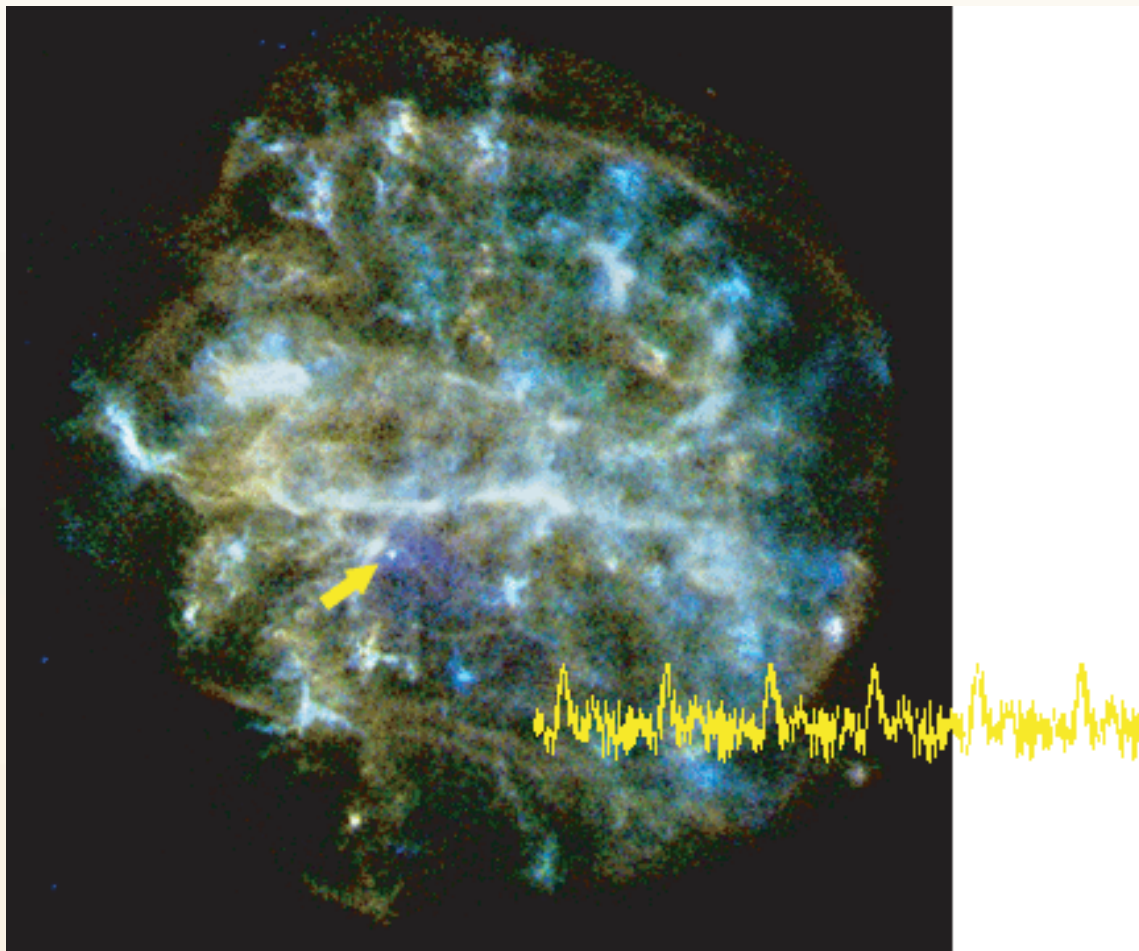
Figure 19 *Chandra X-ray image of the oxygen-rich 1,700 year old composite SNR G292.0+1.8. The position of the pulsar is indicated by the arrow and the mean pulse profile of PSR J1124–5916, obtained from Parkes data, is overlaid.*

Astronomy reports

Discovery of a super-massive spiral galaxy

J. Donley, B. Koribalski (ATNF); R. Kraan-Korteweg (University of Guanajuota, Mexico); A. Schroeder (University of Leicester, UK); L. Staveley-Smith (ATNF) and the ZOA team

How massive can a spiral galaxy become? Current theoretical models predict that spiral galaxies like the Milky Way form from the merger of smaller galaxies at times when the Universe was between 25% and 50% of its current age. This merger process is thought to create a population of present-day spiral galaxies whose number densities decline exponentially at masses higher than a characteristic value, M*. Observational evidence (e.g. from HIPASS, see page 32) support this theory and set M* to a neutral hydrogen (HI) mass of approximately 6×10^9 solar masses. The density of galaxies much more massive than this characteristic value is poorly constrained, however, as these super-massive galaxies are very rare.

Through a large survey that utilised the Parkes multibeam receiver, we have discovered a super-massive spiral galaxy at a distance of 140 Megaparsecs. Data from the Parkes telescope suggest that the galaxy HIZOA J0836–43 has an HI mass of 7×10^{10} solar masses and a total dynamical mass of 1.5×10^{12} solar masses. This HI mass is 20 times that of our own Milky Way Galaxy and the total mass is at least five times the Milky Way's mass! This places HIZOA J0846–43 among the most massive spiral galaxies known, with only a handful of galaxies whose HI and/or total dynamical masses are comparable. Some such galaxies include Malin I, ISOHDFS 27, UGC 1752, UGC 12591, and NGC 1961.

Follow-up high-resolution observations with the Compact Array confirmed that HIZOA J0836–43 is in fact a single system, with a disk radius of 66 kiloparsecs and an inclination-corrected rotational velocity of 312 kilometres per second. The galaxy's rotation curve, the rotational velocity as a function of radius, is constant at large radii. This suggests that, like normal spiral galaxies, HIZOA J0836–43 has a large dark matter halo extending well beyond the disk radius, a property also predicted by current hierarchical clustering models of galaxy formation. This galaxy is so large and massive that, if formed at the very beginning of the Universe, it would only have had time to complete 10 rotations! In addition to giving us insights into the HI properties of HIZOA J0836–43, our observations at the Compact Array have also provided radio continuum data. From these data, we have determined that J0836–43 is probably forming stars at a rate of about 26 solar masses per year.

We have also observed HIZOA J0836–43 with the Anglo-Australian Telescope (AAT) in the near-infrared K and H bands. Because HIZOA J0836–43 is located behind the plane of the Milky Way in a region known as the Zone of Avoidance, the optical B-band emission originating from the galaxy is obscured by nearly 12 magnitudes of dust extinction, preventing us from obtaining an optical image of the galaxy. Luckily, the effect on infrared emission is much less severe than that on the optical light. The AAT observations have therefore allowed us to determine both the inclination of the galaxy, 65 degrees, as well as the distribution of its old stellar population. Both a galactic bulge and disk can be inferred from the infrared emission. The bulge has a central surface brightness of 15 magnitudes per square arcsecond and a scale length of 2 kpc. The disk has a scale length of 4 kpc and can be detected out to a radius of 20 kpc, even through 1 magnitude of extinction in the infrared K band.

The galaxy HIZOA J0836–43 is one of the most massive spiral galaxies ever detected. Although a nearby galaxy can be seen in the AAT image, there is no evidence that the two galaxies are interacting. The velocity field and integrated emission of HIZOA J0836–43 show no disturbances, suggesting that it is a normal, albeit very massive, galaxy. The detection of a super-massive galaxy such as HIZOA J0836–43 helps us to answer fundamental questions that arise when formulating theories of galaxy evolution.

Astronomy reports

Large-scale blind surveys with receivers such as the Parkes multibeam receiver provide one of the best ways to detect such hidden giants.
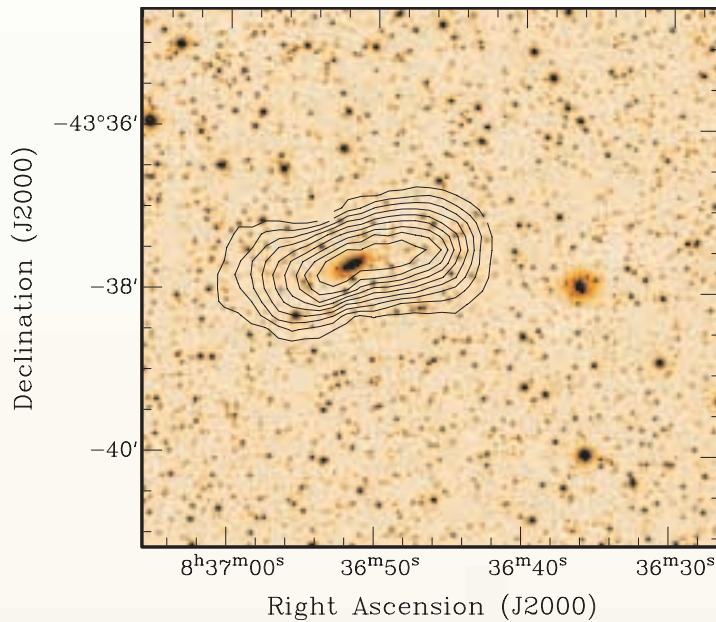
Figure 20 A K-band image of HIZOA J0836–43 from the Anglo-Australian Telescope with the HI contours, obtained from Compact Array data, overlaid. The contour levels show the HI emission from 10% to 90% of the peak value, in increments of 10%.
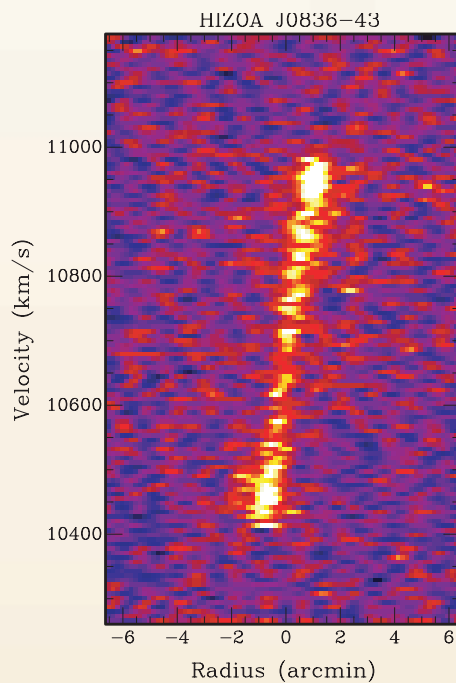
Figure 21 A "position–velocity" diagram for HIZOA J0836–43 along the major axis of the galaxy. The galaxy is seen as the bright strip extending over velocities from approximately 10,400 to 11,000 kilometres per second.

First results from the Compact Array 18 GHz pilot survey

Elaine Sadler (University of Sydney) for the 20-GHz survey team; Roberto Ricci (SISSA, Italy); Ron Ekers, Mike Kesteven, Lister Staveley-Smith, Ravi Subrahmanyan, Warwick Wilson (ATNF); Mark Walker (ATNF/University of Sydney); Carole Jackson (ANU); Gianfranco De Zotti (Padova Observatory, Italy)

In September 2002, as a pilot study for an all-sky radio imaging survey at millimetre wavelengths, we observed 1,216 square degrees of the southern sky at 18 GHz using a novel wideband (4 GHz bandwidth) analogue correlator on one baseline of the Compact Array. Several imaging surveys of the radio sky have already been carried out at frequencies between 0.3 and 5 GHz, where the source population is dominated by powerful radio galaxies and fainter starburst galaxies, but at frequencies above 5 GHz only small areas of sky have been studied in detail. This is mainly because large radio telescopes typically have small fields of view (one to two arcminutes) at high frequencies, making it extremely time consuming to observe large areas of sky. Measuring the high-frequency properties of extragalactic radio sources is crucial for interpreting the high-sensitivity and high-resolution maps of the cosmic microwave background that are now being produced by satellite missions like WMAP and is also important for studies of active galaxies and their cosmic evolution.


The observing team present at Narrabri for the September pilot survey. From left to right: Lister Staveley-Smith, Ron Ekers, Jennifer Donley, Kate Smith, Mike Kesteven, Elaine Sadler, Carole Jackson, Warwick Wilson. In the background, antennas CA02 and CA03 are seen observing the meridian between declinations of –60 and –70 degrees.

The survey is made possible by using the new Compact Array 12-mm receivers in combination with a 4 GHz bandwidth prototype correlator recently developed at ATNF (the standard Compact Array correlator has a bandwidth of 128 MHz). The increased bandwidth means that the continuum sensitivity is high even for short integration times, allowing large areas of sky to be observed in a fast-scanning mode. On 13 – 17 September 2002, we scanned the region of sky between declinations of –60 and –70 degrees using two antennas of the array as a two-element interferometer with the wide-band correlator. We covered roughly 15 square degrees per hour to a detection limit of 60 milliJansky. The Compact Array was used in a "split array" mode, so that regular synthesis imaging could be carried out at the same

time with the antennas which were not being used for fast scanning.

Follow-up radio imaging of the sources detected in the survey was carried out in October 2002, giving more accurate positions and flux densities. Almost half the 226 detected sources lay within five degrees of the Galactic plane, and can be identified with Galactic HII regions, supernovae and planetary nebulae. The remainder are extragalactic sources, made up of candidate quasars (60%), radio galaxies (20%) and faint optical objects or blank fields (20%).

The 18 GHz survey will continue in 2003.
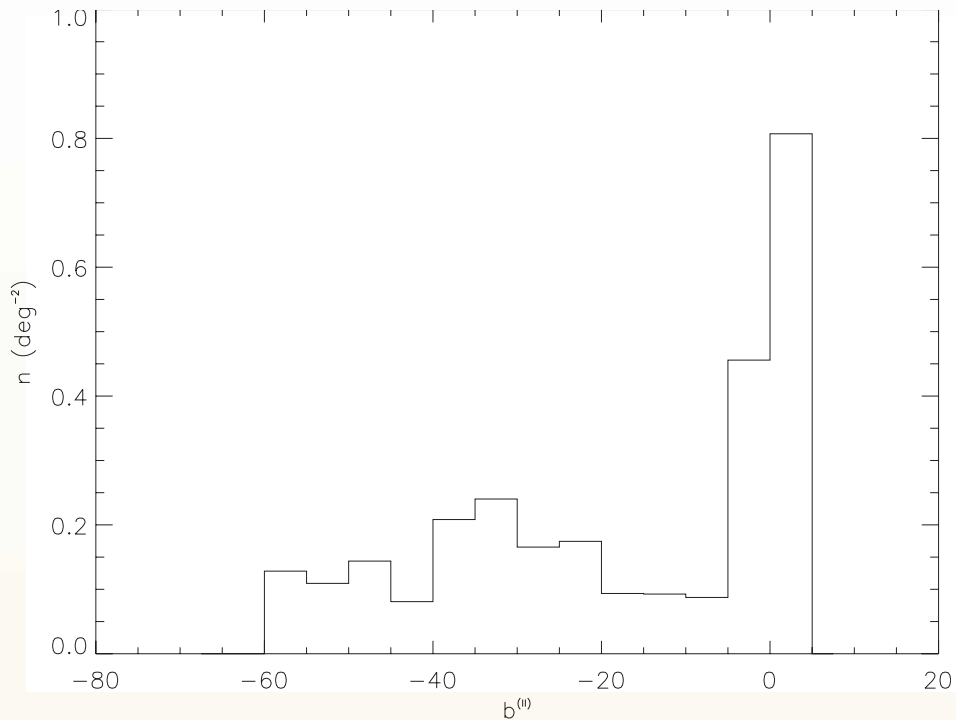
Figure 22 A histogram showing the detected source density from the 18 GHz Pilot Survey in five-degree bins in Galactic latitude. The peak near latitude zero corresponds to the population of Galactic disk sources such as HII regions. The smaller excess at latitudes of –30 to –40 degrees is due to sources associated with the Large Magellanic Cloud.
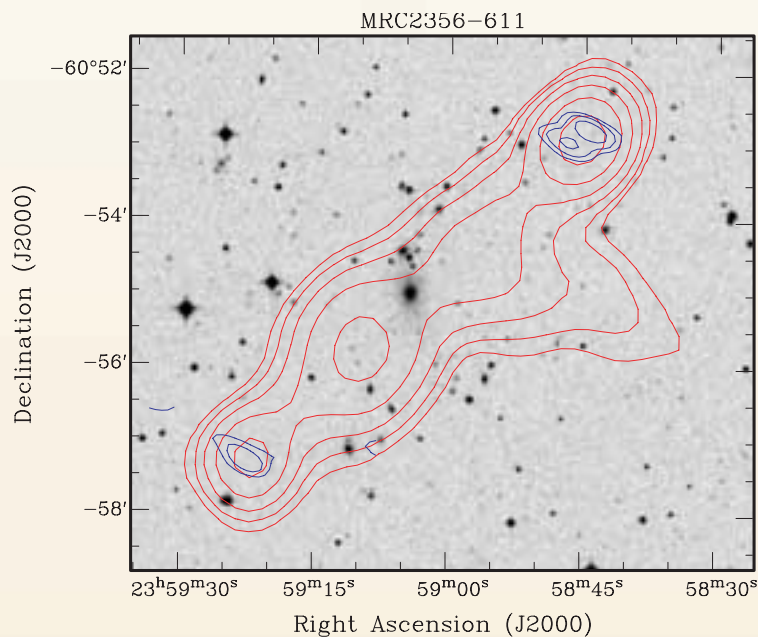
Figure 23 While many of the sources detected in the Pilot Survey are associated with distant quasars, some, like the radio galaxy shown here (an elliptical galaxy at z=0.0963) are relatively nearby. Here the red contours show low-frequency (843 MHz) radio emission from the SUMSS survey. The blue contours show the 18 GHz emission imaged in the Pilot Survey, overlaid on an optical image from the Digitized Sky Survey. The high-frequency radio emission is concentrated at the hotspots (roughly one million light years from the parent galaxy) where relativistic jets of plasma from the galaxy's nucleus terminate and dump their energy.

An unbiased census of hydrogen in the local Universe

M. Zwaan, M. Meyer, R. Webster (University of Melbourne); L. Staveley-Smith, B. Koribalski (ATNF) and the HIPASS team

In 1997 an international team of astronomers set out to survey the entire southern sky for neutral hydrogen (HI) emission using the Parkes radio telescope equipped with the 21-cm multibeam receiver. This instrument is a very efficient survey tool, allowing us to conduct the first large-scale blind neutral hydrogen survey, both in the intermediate neighbourhood of the Milky Way Galaxy, and out to distances of 170 Megaparsecs. The data taking for this survey, known as HIPASS (HI Parkes All Sky Survey), was finished in 2002, and since then much effort has gone into analysing the large dataset. Here, we concentrate on some of the progress that has been made for the extragalactic component of HIPASS.

The HIPASS data consists of 530 cubes, which each cover eight by eight degrees on the sky, and velocities from –1,200 to 12,700 kilometres per second. Together these cubes comprise almost two thirds of the sky, from declination –90 to +25 degrees. So far, most attention has been directed to the 388 southern cubes south of declination 2 degrees. Our first task after creating the data cubes is to identify extragalactic HI 21-cm emission line signals in the noisy background. It was found that this was most efficiently done using two independent automatic finder scripts, the results of which were merged. Galactic high-velocity clouds and detections at frequencies known to be polluted by man-made interference were removed from the list of detections. The remaining 130,000 potential detections were subjected to a series of manual checks for verification by three different individuals. After this process, we were left with approximately 4,300 HI selected galaxies, almost a twenty times larger sample than any existing HI selected sample.

Figure 24 shows the sky distribution of the HIPASS sources. The dashed line at b = 0 indicates the plane of the Galaxy. All optical redshift surveys suffer from severe extinction close to this line, which hinders the identification of extragalactic sources over a large region of sky, and hence leads to an incomplete picture of the large-scale structure of galaxies. The figure clearly shows that HIPASS is not affected by extinction and measures the galaxy distribution equally efficiently in all regions of the sky. This illustrates the power of HIPASS to study the large-scale structure in the local Universe.

A more quantitative analysis of the large-scale structure is possible with a tool known as the two-point correlation function. This measures the excess probability of finding another galaxy at a given distance from any galaxy in the sample. For optically selected galaxies, this function has been studied extensively and has been shown to be dependent on galaxy luminosity, morphological type, and star formation activity. Figure 25 shows a two-dimensional form of the correlation function of HIPASS galaxies. The vertical and horizontal axes correspond to separations between galaxies orthogonal and parallel to the line of sight, respectively. Integrating along vertical lines, and applying some mathematics, finally leads to a measurement of the real space correlation function, which is shown in Figure 26. For comparison, the correlation function from the 2dF galaxy redshift survey, at the Anglo-Australian Telescope (AAT), of optically selected galaxies is also shown. This diagram shows that our sample of HI-selected galaxies, representing a population of more slowly evolving galaxies, is less strongly clustered than the optically-selected sample. Possibly, two effects are at play here. These gas-rich galaxies might only survive in regions without too many interactions with neighbouring galaxies, which could trigger star formation and burn up the HI. Another explanation is that the HI-rich galaxies are actually formed in lower density regions.

Astronomy reports

Apart from studying the large-scale structure, HIPASS is useful for measuring exactly how HI is distributed over galaxies of different masses. An analysis of one of the first products of HIPASS, the Bright Galaxy Catalogue containing the 1,000 brightest detections, resulted in the most accurate measurement of the HI mass function to date. This new HI mass function is in good agreement with earlier, much poorer determinations, and allows for a precise evaluation of the neutral gas mass density at the present epoch. Expressed as a fraction of the critical density of the Universe, the neutral gas mass density is only 0.038%. This is approximately five times lower than at the time when the Universe was only 10% its present age, indicating the gradual conversion from neutral gas to stars in the disks of galaxies.
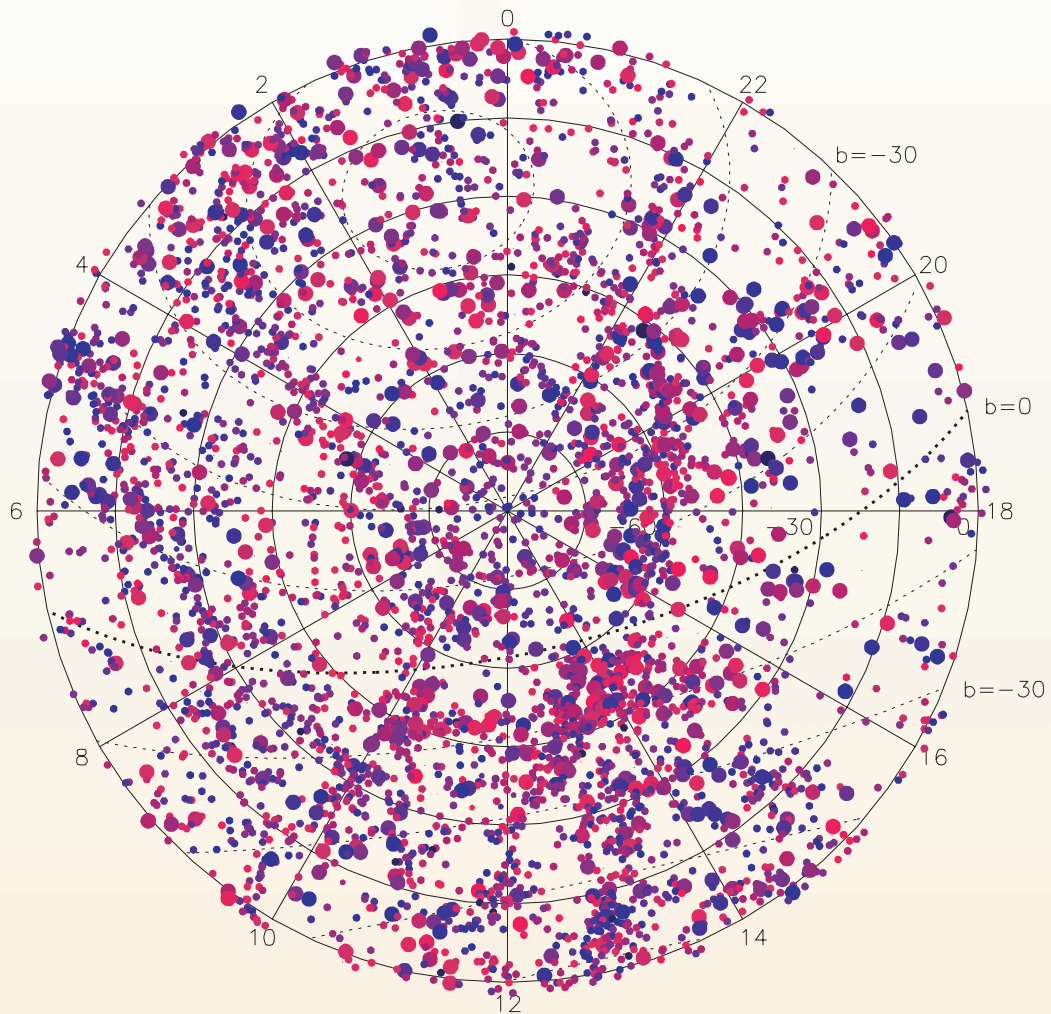
Figure 24 *The distribution of extragalactic HIPASS sources in the southern skey. The colour coding corresponds to the distances of the sources, in the sense that redder colours correspond to higher distances. The symbol size indicates the neutral hydrogen mass of the sources. The dashed line marked with b = 0 is the Galactic plane. The south celestial pole is in the centre of the image.*
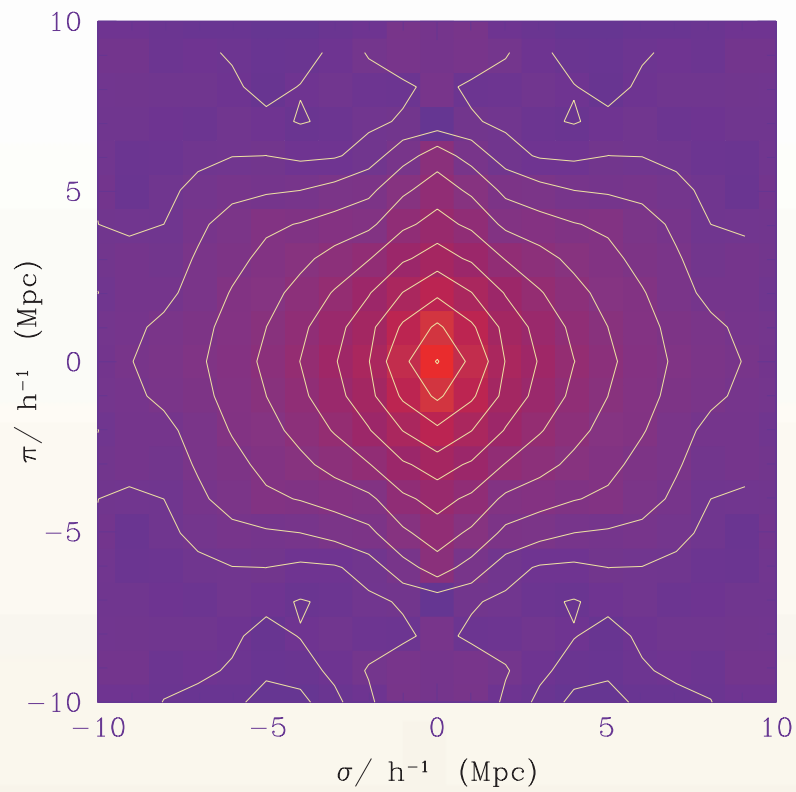
Figure 25 *The two-point correlation function for HIPASS galaxies, plotted as a function of transverse (σ) and radial (π) pair separation.*
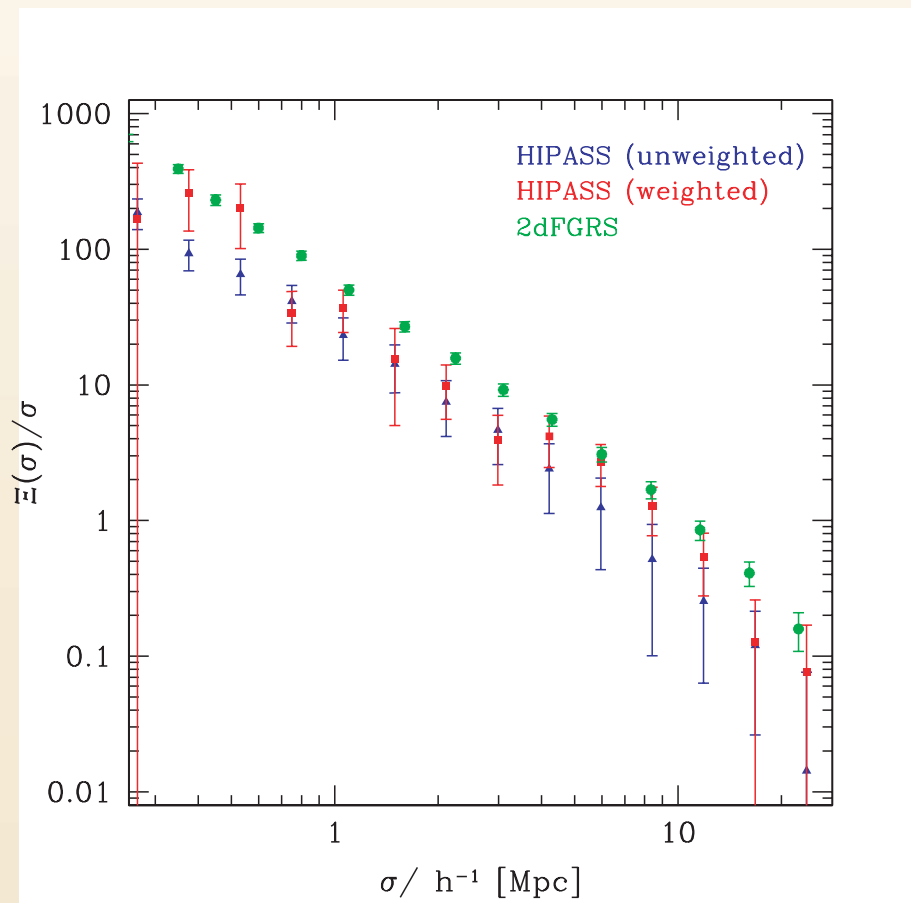
Figure 26 *The projected real space correlation function for HIPASS and 2dF galaxies. The HI-selected galaxies are less strongly clustered than galaxies found in the 2dF galaxy survey.*

The Southern Galactic Plane Survey

N. McClure-Griffiths (ATNF); J. Dickey (University of Minnesota, USA); A. Green (University of Sydney);
*B. Gaensler (Harvard University, USA)*

The Milky Way provides the closest laboratory for studying the physics of the interstellar medium (ISM). Despite some 50 years of studies with radio telescopes, our knowledge of the dynamics and thermodynamics of the atomic phase of the ISM is remarkably limited. However, for the past five years the ATNF has been involved in a large-scale survey of the ISM in the Southern Milky Way. This project, the Southern Galactic Plane Survey (SGPS), aims to image the 21-cm continuum emission and atomic hydrogen spectral line in a region of 335 square degrees in the plane of the Milky Way. The first part of the survey, SGPS I, covered an area of 210 square degrees centred on the Galactic midplane (Galactic latitudes –1 to +1 degrees), spanning Galactic longitudes from 253 to 358 degrees. In 2002 we began a second phase, SGPS II, which covers a 100 square-degree region around the Galactic Centre and extends along the Galactic midplane to longitude +20 degrees. The SGPS II is in progress, with completion anticipated in mid-2004.

The SGPS constitutes more than an order of magnitude improvement in both angular resolution and sensitivity over previous surveys of this region. Additionally, the combination of high-resolution data from the Compact Array and short spacing information from the Parkes radio telescope provides a dataset that is sensitive to all angular scales from two arcminutes to several degrees, as illustrated in Figure 27. The general goals of the survey are to understand the structure, dynamics, and thermal distribution of the neutral hydrogen component of the ISM. We also have full polarisation information in the continuum that we are using to study the magnetic field structure of the Milky Way and the magneto-ionic medium. The SGPS data has been combined with two surveys of the northern hemisphere Galactic plane made with telescopes in Canada, the USA, and Germany to form the International Galactic Plane Survey. The ultimate goal of this collaboration is to construct an atlas of the HI in the entire Galactic plane with an angular resolution of one arcminute, a spectral resolution of one kilometre per second and a sensitivity limit of one Kelvin.

The SGPS is producing many new and exciting results. The work includes studies of HI shells, bubbles and chimneys (including the one on the cover of this report), which are some of the largest objects in the ISM. These objects, which are believed to be formed by the combined effects of stellar winds and supernovae, can break out of the Galactic plane and expel hot gas from the disk into the halo. The chimney shown on the cover, GSH 277+00+36, was discovered in the SGPS I; it is more than 600 parsecs in diameter and extends over a kiloparsec above and below the Galactic plane. Along the walls of this shell we have detected gas instability structures on scales of only a few parsecs. It is through these instabilities that gas returns to the cool phase and these may account for much of the small scale structure in the ISM.

Using data from the entire SGPS I region we have created a new longitude–velocity diagram of HI emission, shown in Figure 28. We combine almost 10,000 spectra for this high-resolution image of HI in the plane. These data allow us to trace spiral features out to Galactic radius 30 kiloparsecs. There are a number of interesting features in this image. At large, positive velocities (<100 kilometres per second) we detect the edge of the HI disk as a thin ridge of emission. This may be a distant extension of the outer spiral arm.

From the SGPS data we have measured the rotation curve of the inner Galaxy, shown in Figure 29. This is the most densely sampled HI rotation curve ever produced; it shows a number of new results. In particular we see strong departures from smooth circular rotation associated with the spiral arms, which are marked with dotted lines. According to spiral density wave theory we expect that gas approaching a spiral arm from the inner Galaxy side should show a decrease in circular velocity before the arm and then an increase as the gas passes through the arm. This is almost exactly what we see in the Milky Way.
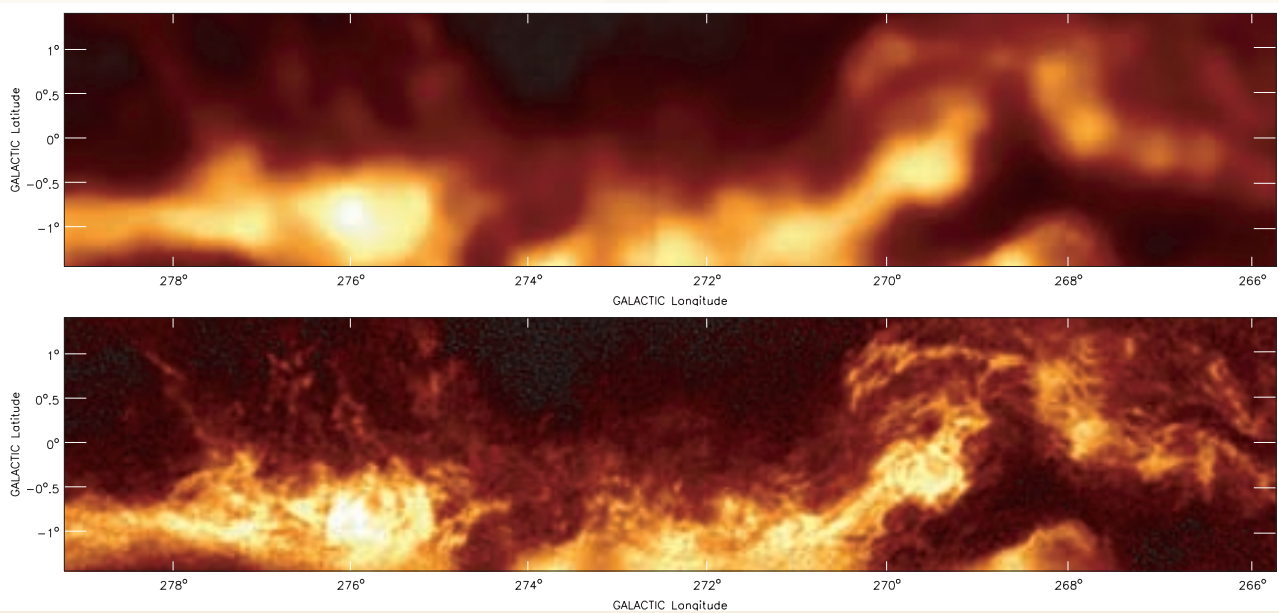
Figure 27 A cross-section of the Milky Way as seen at a wavelength of 21 cm. The upper figure is an image made by the Parkes telescope with the multibeam receiver observing the 21 cm line with an angular resolution of 14 arcminutes. The area covered is from Galactic longitudes of 266 to 280 degrees, and latitudes of –1.5 to +1.5 degrees at a local standard of rest velocity of +73 kilometres per second. The lower image shows the same area as seen with a combination of Parkes plus Compact Array data, with an angular resolution of 2 arcminutes. In both images, the light yellow colour corresponds to bright emission from atomic hydrogen, while black shows no emission. This velocity plane traces the outer Galaxy, far outside the solar circle, where the disk is warped toward negative latitudes in this longitude range (note that the bright ridge does not align with zero latitude). The broad, dark channel that bisects the disk on the right-hand side is a superposition of many giant shells resulting from stellar winds and explosions.
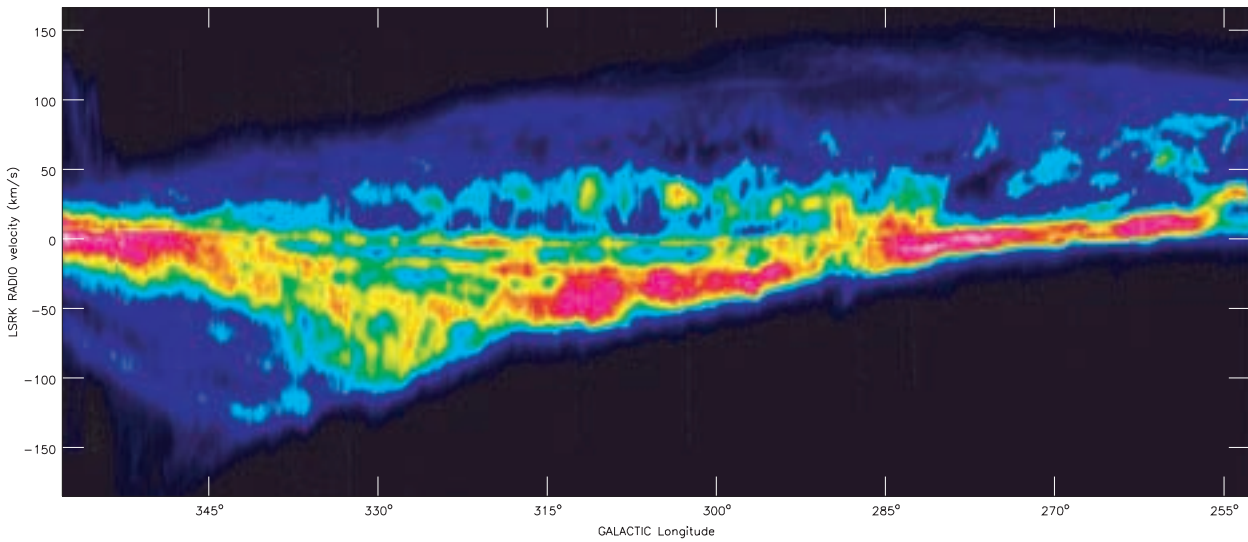
Figure 28 *Longitude–velocity image of the HI emission in the Galactic plane over the entire SGPS I region. There are approximately 10,000 pixels along the longitude axis. Positive velocities correspond to gas outside the solar circle, whereas negative velocities show gas in the inner Galaxy. Using this image we can search for the outer edge of the HI disk (at large positive velocities). We are also able to trace the outermost spiral arms. The Sagittarius-Carina spiral arm is apparent as a loop of strong emission (very pink) crossing near longitude 280 degrees.*
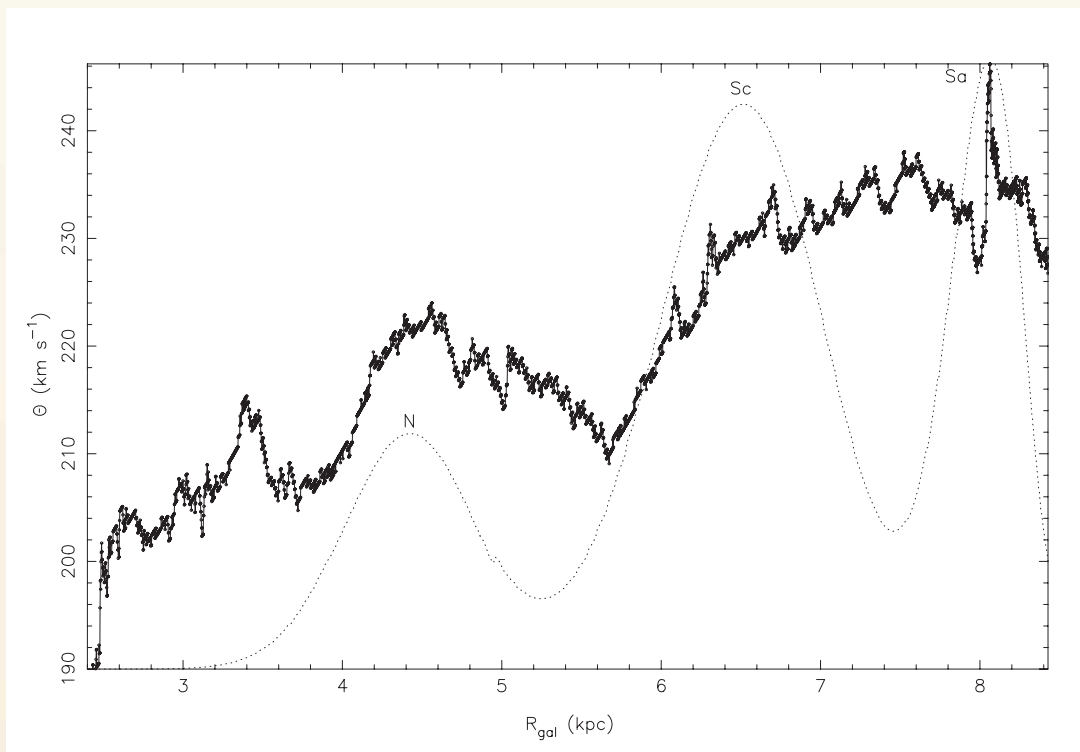
Figure 29 *HI rotation curve for the inner Galaxy (fourth quadrant), sampled every arcminute. The dotted line shows the approximate positions and widths of the spiral arms which are labelled from left to right as Norma arm (N), Scutum-Crux arm (Sc) and the Sagittarius-Carina arm (Sa). The rotational velocity decreases as the gas enters a spiral arm and then begins to increase as the gas passes through the arm.*